Momentum transport in MAST spherical tokamak plasmas

A. R. Field, R. J. Akers, N. J. Conway, [1]M-D. Hua, M. Wisse

EURATOM/UKAEA Fusion Association, Culham Science Centre,
Abingdon, Oxon, OX14 3DB, UK
[1]Imperial College, University of London, London, UK.

Introduction

Confinement in magnetically confined plasmas is influenced by the transport of toroidal angular momentum. This is because the plasma rotation often makes the dominant contribution to the E×B flow shear, which can be sufficient to reduce the level of anomalous transport. The low moment of inertia of spherical tokamak plasmas results in high rotation rates with tangential NBI heating, the rotation scaling expected to scale as $\varepsilon^{-1.4} R^{-2}$, where ε is the inverse aspect ratio a/R (under the assumptions of a fixed ratio of momentum to energy confinement time and the IPB(y, 2) energy confinement scaling). In MAST the tangential NBI heating beams consequently drive strong toroidal rotation with $\omega_\phi \sim 1$-3×10^5 s^{-1} and toroidal Mach number $M_\phi = R\omega_\phi / v_{th,i} \sim 0.3$-$0.8$, which is sufficient to suppress the ion-scale anomalous transport in the mid-radius region of the plasma [1].

Transport analysis of MAST plasmas performed using TRANSP is based on data from a suite of kinetic profile diagnostics, including electron density and temperature from a 200 Hz NdYAG TS system and T_i and ω_ϕ from multi-channel CXRS with spatial resolution of order of the ion Larmor radius, ρ_i. Z_{eff} profiles are also obtained from a 2D bremsstrahlung imaging diagnostic. Data from these diagnostics are mapped onto the magnetic equilibrium from EFIT and combined in a self-consistent manner using an integrated analysis chain (MC^3) to provide self-consistent input data for subsequent transport analysis using TRANSP [2].

Here, results are presented from experiments comparing plasmas heated by two different designs of beam source, which operate at different energies and thereby delivering different levels of torque and also ratio of electron to ion heating at a given power. This difference is found to have a significant effect on the plasma transport properties. The relation between the ion thermal transport and the momentum transport is also quantified in terms of the Prandtl number P$_\phi$ (the ratio of the momentum to the ion thermal diffusivities χ_ϕ / χ_i) from transport analysis of a number of well diagnosed MAST discharges.

Source Comparison

The applied torque from the NBI sources is given approximately by $T_B = P_B R_B (2m_i / eE_B)^{1/2}$, where P_B is the beam power R_B is the beam tangency radius and E_B is the injection energy (here neglecting the contribution from the half and third energy components for simplicity). For a given injected power, the applied torque is thus higher with lower energy beams. During 2006 MAST operated with different sources on the two beam lines of which the ORNL 'duo-pigatron' source was typically operated at lower injection energy than the JET style, PINI source for a given injected power. For example at 1.5 MW injected power the ORNL source operates at 48 keV and the PINI at 60 keV hence the former delivers a factor ~ 1.13 larger torque to the plasma. This facility has been used to perform experiments to investigate directly the influence of the variation of the applied torque and electron/ion heating ratio on otherwise similar plasmas with the same applied heating power. The co-injected, L-mode DND discharges were of 740 kA plasma current, 0.57 T toroidal field, line-average density of $\leq 2.5\times10^{19}$ m^{-3} with a stored energy of ~ 70 kJ.
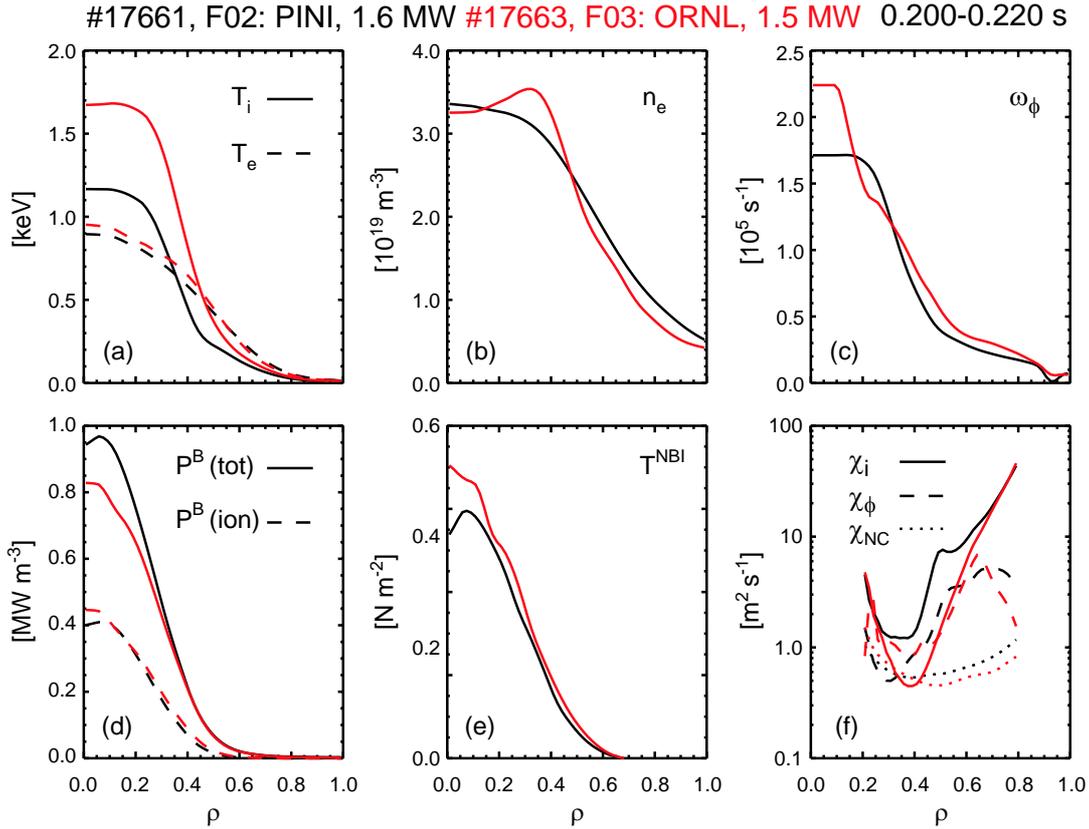
Fig. 1 Comparison of similar L-mode discharges heated by different NBI sources (PINI (black), 1.6 MW at 60 keV or ORNL (red), 1.5 MW at 48 keV). Profiles are shown of (a) $T_{i,e}$, (b) n_e, (c) ω_ϕ, (d) NBI power density P^B(total and to ions), (e) NBI torque density T^{NBI} (including from fractional-energy beam components) and (f) ion thermal χ_i and momentum χ_ϕ diffusivities and the neo-classical χ_i^{NC} from NCLASS.

In Fig. 1 profiles of these discharges are shown averaged over a 20 ms period of the flat-top phase. The electron temperature and density profiles in the discharges are similar, with $T_e \leq 1$ keV. In the discharge heated by the lower energy ORNL source the ion temperature is significantly higher ($T_i \leq 1.7$ keV) than in the plasma heated by the PINI source ($T_e \leq 1.2$ keV). Similarly, in the gradient region the rotation is also somewhat higher with the lower injection energy. This difference is notable considering that the total injected power is slightly higher (1.6 MW) from the 60keV beam from the PINI than the 1.5 MW from the 48 keV ORNL source. The NBI power deposition profiles are similarly peaked, with approximately equal powers to the ions and electrons, although there is ~ 15% more heating to the electrons with the higher energy beam. Including the Ohmic heating and the ion-electron exchange heating, the total power to the electrons is about twice that to the ions in both cases. The torque density profiles are also peaked with about a factor 12% larger torque from the lower energy beam. Typically, in L-mode discharges χ_i exhibits a minimum in the mid-radius region, where the ion thermal transport approaches the neo-classical level. In the discharge with the lower energy beam with higher T_i and ω_ϕ this minimum in χ_i is consequently more pronounced, with $\chi_i \sim \chi_i^{NC}$ and at slightly broader radius. The toroidal momentum diffusivity χ_ϕ, which is defined below, is of a similar magnitude to χ_i. The effective neo-classical momentum diffusivity χ_ϕ^{NC} calculated from an appropriate theory [3], including the effect of strong rotation is at least an order of magnitude smaller than the observed value.

Momentum transport

Previous studies on several tokamaks have shown momentum and ion thermal transport to be closely linked, with the momentum confinement time comparable to the energy confinement time. On ASDEX [4] and DIII-D [5] Prandtl number $P_\phi = \chi_\phi / \chi_i$ was found to be of order unity, although studies on JET [6] have found this ratio to be significantly below unity with $0.18 < P_\phi < 0.35$. Theoretical studies of ITG transport [7, 8] predict a close coupling of momentum and ion heat transport with $P_\phi = 1$. More recent studies, however, predict a turbulent momentum pinch [9] and the interpretation of NBI modulation experiments on JET [10] yield $P_\phi \sim 1$ provided an inward momentum pinch $v_{\phi,pinch} \sim 8\text{-}15 \text{ ms}^{-1}$ is accounted for in the analysis. Non-resonant magnetic braking experiments on NSTX [11] also show the presence of an inward momentum pinch with $v_{\phi,pinch} \sim 30 \text{ ms}^{-1}$, although on this device χ_ϕ is typically significantly less than χ_i under steady state conditions.

The toroidal angular momentum density of the plasma is defined as $l_\phi = m_i n_i \langle R^2 \rangle \omega_\phi$ and its rate of change is expressed by the momentum balance as:

$$\frac{d}{dt}(l_\phi) = \nabla \cdot \Gamma_\phi + T_\phi \tag{1}$$

where Γ_ϕ is the viscous momentum flux defined as $\Gamma_\phi = -m_i n_i \langle R^2 \rangle \chi_\phi d\omega_\phi / dr$, where χ_ϕ is the toroidal momentum diffusivity and T_ϕ is the applied toroidal torque, which may include MHD induced torques as well as that from the NBI heating. The effective value of χ_ϕ is determined from TRANSP analysis using the measured kinetic data and the NBI torque determined from a Monte Carlo beam model. This value will include contributions from both neo-classical and turbulent momentum fluxes but does not allow for the presence of a momentum pinch. The presence of a momentum pinch can only be determined from perturbative experiments with time-dependent braking applied from external magnetic perturbations or modulated torque from the NBI heating. In future it will be possible to perform braking experiments using the internal ELM control coils now installed in MAST.

Data from transport analysis of a number (19) of MAST L- and H-mode discharges with both
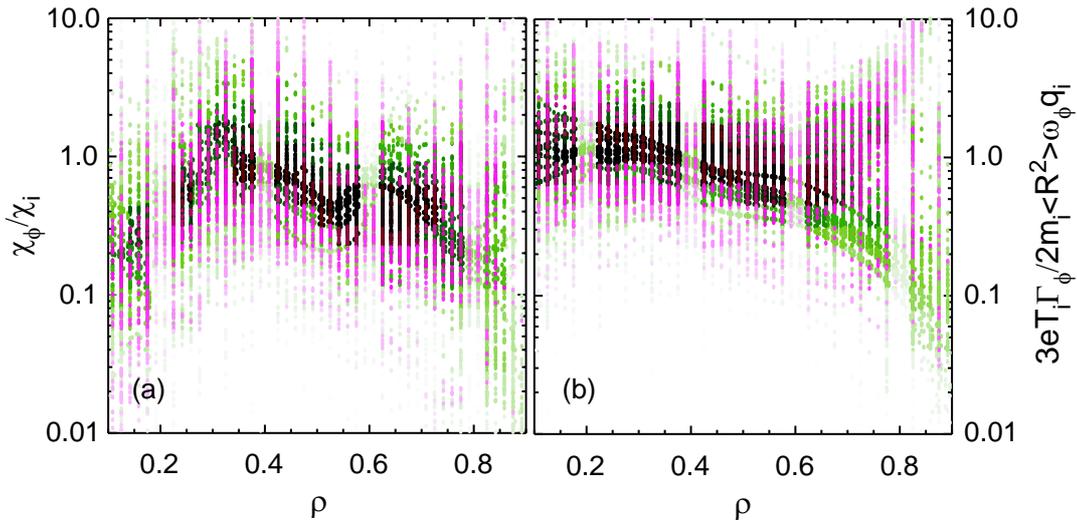

Fig. 2 Plots of (a) the Prandtl number χ_ϕ/χ_i and (b) the ratio of the normalised momentum flux $\Gamma_i / n_i m_i \langle R^2 \rangle \omega_\phi$ to the normalised ion heat flux $2q_i / 3n_i T_i$ at many times during a number of L- (green) and H-mode (magenta) discharges as a function of normalised radius.

co- and counter-NBI heating has been combined to investigate any common trends in the transport coefficients. The discharges have nominally 800 kA plasma current, 0.8-2.1 MW beam power and line-average density in the range $2\text{-}4\times10^{19}$ m^{-3}. One striking result of this analysis is the robustness of the Prandtl number profile. Data from all valid times during the flat-top phases of these discharges are shown in Fig 2, where the intensity of colour represents the density of data points and the H-mode data is shown in magenta and the L-mode data in green. Although there is appreciable scatter in the data P$_\phi$ varies between about 1.0 in the core to about 0.3 in the outer region with little appreciable difference in behaviour between the L- and H-mode phases. This indicates that there may be a common property of the anomalous transport relating the level of momentum to heat transport between these regimes.

The Prandtl number is related to the ratio of the normalised ion heat flux $2q_i/3n_iT_i$ to the normalised angular momentum flux $\Gamma_i/n_i m_i\langle R^2\rangle\omega_\phi$ through the ratio of the scale lengths of the rotation frequency L_ω and the ion temperature L_{T_i} according to:

$$\frac{\chi_\phi}{\chi_i}\cdot\frac{L_{T_i}}{L_\omega} = \frac{3/2\,eT_i}{m_i\langle R^2\rangle\omega_\phi}\cdot\frac{\Gamma_\phi}{q_i} \tag{2}$$

This normalised ratio is shown in Fig 2(b) for comparison with the plot of the Prandtl number profile. Whereas there is no discernable difference in P$_\phi$ profile between the L- and H-mode discharge phases, there is a distinct difference in the profile of the normalised flux ratio. In H-mode there is a relatively larger level of momentum flux compared to heat in the ion channel in the outer part of the profile. This can be attributed to a larger ratio L_{T_i}/L_ω in this region in H-mode compared to L-mode, i.e. a relatively stronger rotation gradient in the outer regions.

Summary

Strongly sheared toroidal rotation is a dominant factor in determining the transport properties of NBI heated ST plasmas. Heating with lower energy beams deposits more torque and ion heating and consequently can produce a stronger, broader ion transport barrier. Momentum transport is closely related to ion thermal transport with the ratio of momentum to ion thermal diffusivities of order unity, neglecting a possible contribution from a momentum pinch which cannot be ruled out without performing dedicated perturbative experiments.

References:

[1] A. R. Field, R. J. Akers, C. Brickley, et al., EX/P2-11 in Proc. 20th IAEA FEC, Vilamoura, Portugal, 2004.
[2] R.J. Hawryluk, Physics of Plasmas Close to Thermonuclear Conditions, (CEC, Brussels, 1980), Vol. 1, p. 19
[3] S. Newton, P. Helander, Phys. Plasmas, **13** (2006) 012505.
[4] A. Kallenbach et al., Nucl. Fusion **33** (1991) 595.
[5] J.S. deGrassie, D.R. Baker, K.H. Burrell et al., Nucl. Fusion **43** (2003) 142.
[6] P. C. deVries, K. M. Rantamäki, C. Giroud et al., PPCF **48** (2006) 1693.
[7] N. Mattor, P. Diamond, Phys. Fluids **31** (1988) 1180.
[8] A.G. Peeters, C. Angioni A. Bottino et al., PPCF **48** (2006) B413.
[9] A. G. Peeters, C. Angioni, D. Strintzi, Phys. Rev. Lett. **98** (2007) 265003.
[10] T. Tala, K. Krombe, P. C. deVries et al., PPCF **49** (2007) B291.
[11] S. Kaye, W. Solomon, R.E. Bell, et al., Bulletin of APS, **52** 16 (2007) 61.